Ventral tegmental area GABA neurons integrate positive and negative valence

Margaret E. Stelzner[1,2,3], Amy R. Wolff, PhD[1,2], Benjamin T. Saunders PhD[1,2]

[1] Department of Neuroscience, University of Minnesota
[2] Medical Discovery Team on Addiction, University of Minnesota
[3] Graduate Program in Neuroscience, University of Minnesota

Correspondence: BTS (bts@umn.edu, saunderslab.com)

PREPRINT

Ventral tegmental area (VTA) dopamine (DA) neurons are classically linked to Pavlovian reward learning and reinforcement. Intermingled VTA GABA neurons are positioned to regulate dopaminergic and striatal systems, but we lack critical insight into how this population contributes to conditioned motivation in different learning contexts. Recording DA and GABA neurons across multiple conditioning paradigms, we found that GABA neurons not only actively encode appetitive and aversive cues and outcomes separately, but uniquely integrate salient events of both valences to guide reward seeking.

The Ventral tegmental area (VTA) is centrally involved in learning and reinforcement (Berke, 2018; Cox & Witten, 2019; Howe & Dombeck, 2016; Schultz, 2006; Sharpe et al., 2017; Tsai et al., 2009). Classically, VTA dopamine (DA) neurons encode cue-outcome associations with increased activity to positively valenced events and decreased activity to negatively valenced events (Cohen et al., 2012; Day et al., 2007; Keiflin et al., 2019; Keiflin & Janak, 2015; Morales & Margolis, 2017; Saunders et al., 2018; Schultz, 2016; Steinberg et al., 2013). The VTA, however, is a heterogeneous region and also contains a substantial population of GABAergic neurons that are less understood (Breton et al., 2019; Nair-Roberts et al., 2008; Swanson, 1982). VTA GABA neurons were long thought to represent an "anti-reward" signal because of their ability to inhibit local DA neurons (Tan et al., 2012; van Zessen et al., 2012). Growing evidence has complicated this notion, demonstrating a role for VTA GABA neurons in behavioral flexibility, motivation, and reward (Al-Hasani et al., 2021; Bouarab et al., 2019; Cohen et al., 2012; Eshel et al., 2015; Hughes et al., 2019; Kim et al., 2010; Lefner & Moghaddam, 2024; Zhou et al., 2022; Wakabayashi et al., 2019), with inconsistent evidence of the active role of these populations in appetitive versus aversive contexts. Critically, there remains a dearth of direct comparisons between genetically identified VTA DA and GABA neuron encoding, and a lack of assessment of these populations in multi-valent learning contexts, where unique motivational resources are marshalled to promote decision-making under conflict.

To address these questions, we selectively targeted DA or GABA neurons of the VTA with GCaMP8f (**Fig. 1A-C; Supplemental Fig. 1**) and recorded calcium fluorescence as a proxy for *in vivo* neural activity in freely moving rats engaged in various Pavlovian learning paradigms. We find that, in contrast to DA neurons, GABA neurons not only actively encode both appetitive and aversive cues and outcomes, but also integrate events of both valences to guide reward seeking. Our results support an evolution of the computational landscape for the VTA, where distinct populations of neurons act in parallel to signal different aspects of motivation under various behavioral conditions.

We first trained rats on a Pavlovian reward conditioning paradigm in which a conditioned stimulus (CS+) predicted reward delivery (liquid Ensure) and a distinct neutral stimulus (CS-) had no paired outcome (**Fig. 1D**). Rats reliably distinguished between the stimuli by the end of training and selectively approached the reward port in response to the CS+ (**Fig. 1E, F**). We found no behavioral differences across sex or neuronal recording groups (**Supplemental Fig. 2**). In contrast
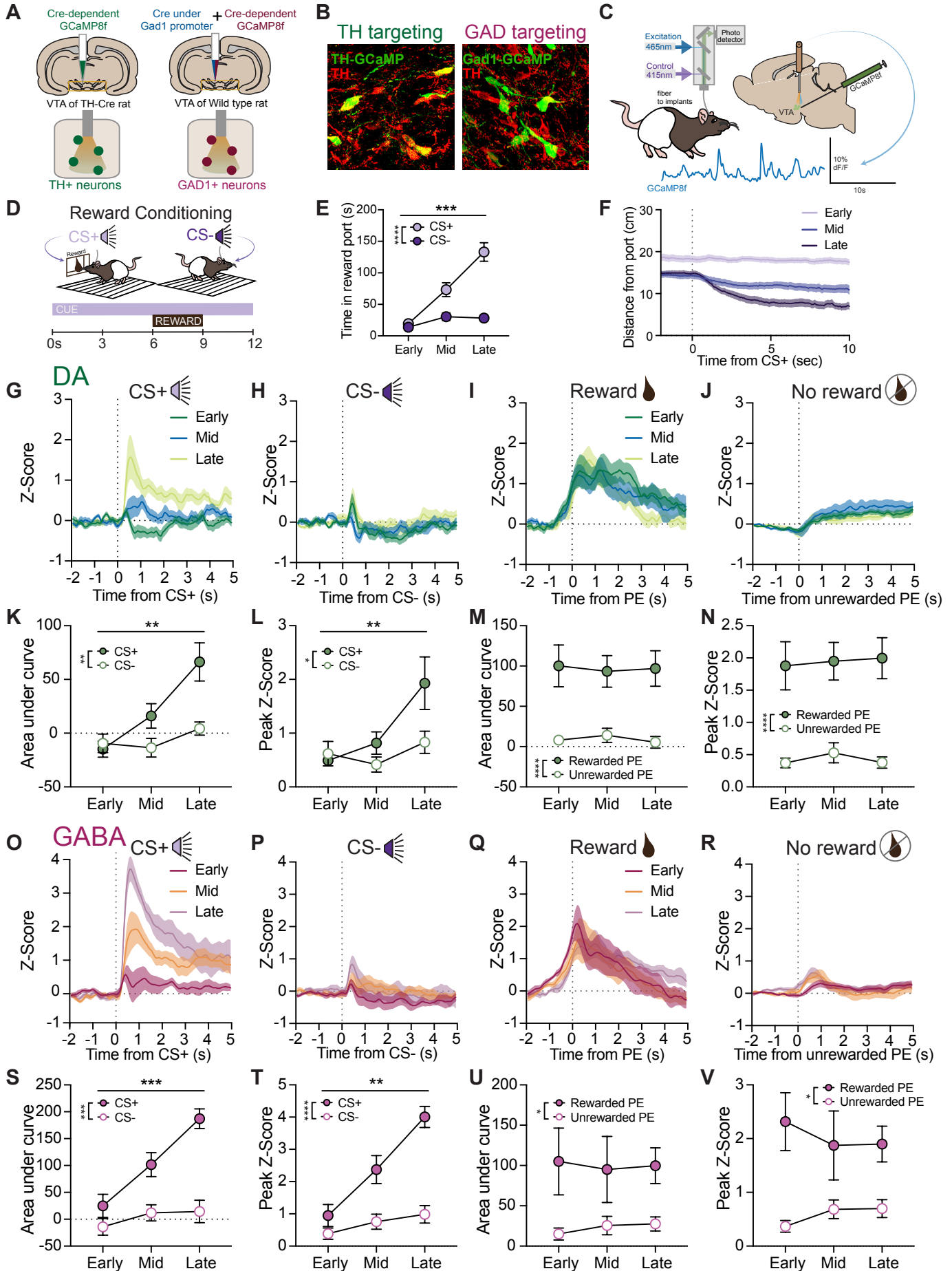
Fig 1 | Conditioned and unconditioned appetitive events are similarly encoded by VTA DA and GABA neurons

A) Approach for cell-type specific targeting with DA neurons targeted through a TH-cre transgenic line and GABA neurons targeted with a viral delivery of cre to GAD1+ neurons. **B)** Examples of viral expression in the VTA. **C)** Schematics of fiber photometry approach, and **D)** experimental design. Rats received cue (CS+) + reward (Ensure) pairings and a distinct neutral cue (CS-) that did not have a paired outcome, while recording VTA GCaMP signals with fiber photometry. **E)** Rats (n=19; 8F, 11M) learned to discriminate the two cues as measured by time spent in reward port during conditioned stimuli presentations across training (two-way ANOVA, cue-type main effect, $F_{(1,36)}=20.94$, $p<0.0001$; interaction $F_{(2,66)}=12.92$, $p<0.0001$). **F)** As rats learned, they approached the magazine rapidly after CS+ onset. **G-N)** Calcium recordings from VTA DA neurons (n=11; 4F, 7M). **G)** DA neurons developed robust activity in response to the CS+ cue, **H)** while showing minimal responses to the CS- cue. **I)** Reward consumption evoked consistent DA neuron activity across training, **J)** while unrewarded port entries (PEs) were associated with minimal DA activity. **K)** DA neuron activity strongly discriminated CS+/CS- cues as training progressed, as measured by AUC (two-way repeated measures ANOVA: session by cue interaction, $F_{(1.77,17.67)}=7.19$, $p=0.0065$; main effect of cue, $F_{(1,10)}=10.24$, $p=0.0095$) and **L)** peak (session by cue interaction, $F_{(1.95,19.45)}=8.587$, $p=0.0023$; main effect of cue, $F_{(1,10)}=5.016$, $p=.049$) measures of the GCaMP signal. **M)** DA neuron activity strongly discriminated rewarded versus unrewarded PEs consistently across training for both AUC (session by response type interaction, $F_{(1.47,14.7)}=.1531$, $p=.795$; effect of response type, $F_{(1,10)}=41.12$, $p<.0001$) and **N)** peak (session by response type interaction, $F_{(1.47,14.65)}=.134$, $p=.812$; effect of response type, $F_{(1,10)}=58.51$, $p<.0001$) signal measures. **O-V)** Calcium recordings from VTA GABA neurons (n=8; 4F, 4M). **O)** GABA neurons developed robust activity to the CS+ cue, **P)** while showing minimal responses to the CS- cue. **Q)** Reward consumption evoked consistent GABA neuron activity across training, **R)** while unrewarded PEs were associated with minimal GABA activity. **S)** GABA neuron activity strongly discriminated CS+/CS- cues as training progressed, as measured by AUC (two-way repeated measures ANOVA: session by cue interaction, $F_{(1.88,13.19)}=16.89$, $p=.0003$; main effect of cue, $F_{(1,7)}=58.66$, $p=.0001$) and **T)** peak (session by cue interaction, $F_{(1.58,11.1)}=12.29$, $p=.0023$; main effect of cue, $F_{(1,7)}=79.37$, $p<.0001$) measures of the GCaMP signal. **U)** GABA neuron activity also strongly discriminated rewarded versus unrewarded PEs consistently across training for both AUC (session by response type interaction, $F_{(1.71,11.96)}=.2605$, $p=.855$; effect of response type, $F_{(1,76)}=5.606$, $p=.049$) and **V)** peak (session by response type interaction, $F_{(1.44,10.1)}=.1589$, $p=.246$; effect of response type, $F_{(1,7)}=8.432$, $p=.023$) signal measures. Data reflect subject means +/- SEM. $*p<0.05$, $**p\leq 0.01$, $***p\leq 0.001$, $****p\leq 0.0001$.

to classic notions that GABA neuron activity opposes DA neurons, we found that robust CS+-evoked activity emerged in both DA and GABA neurons as learning progressed (**Fig. 1G, O**), and activity consistently increased to reward throughout conditioning in both neural subtypes (**Fig. 1I, Q**). Both DA (**Fig. 1G-N**) and GABA (**Fig. 1O-V**) signals also strongly discriminated CS+ from CS- presentations and unrewarded PEs, which elicited minimal calcium responses. The similarity in appetitive event encoding between DA and GABA neurons clarifies their parallel, as opposed to merely oppositional, roles in reinforcement learning.

In prevailing frameworks, DA neurons are inhibited by aversive stimuli, potentially via activity of local GABA neurons (Cohen et al., 2012; Schultz, 2016; Tan et al., 2012). Other findings, however, demonstrate that VTA DA neurons can play an active role in Pavlovian threat and punishment encoding (Brischoux et al., 2009; Cai et al., 2020; Jo et al., 2018; Park & Moghaddam, 2017). It therefore remains unclear how these populations directly compare in their participation in aversive learning.

To compare DA and GABA neurons in the same aversive stimulus context, we next trained rats on a fear conditioning paradigm, with presentations of a conditioned stimulus predicting a moderate footshock (CS+) and a neutral stimulus (CS-) (**Fig. 2A**). Rats learned to distinguish the two cues as measured by their freezing behavior (**Fig. 2B**). In contrast to reward conditioning, VTA DA neurons showed minimal response to the onset of the shock CS+ and the shock

itself (**Fig. 2C-J**), and these signals did not change relative to the initial cue habituation session. A small increase in DA neuron activity was evident at the point of shock offset, and the offset of the CS- (**Fig 2E, F, I, J**). In contrast, GABA activity strongly increased in response to shock itself (**Fig. 2M, Q, R**) and rapidly came to signal the onset of the cues during conditioning, generalizing between the CS+ and CS- (**Fig. 2K, L, O, P**). These data help resolve ongoing debates to indicate that VTA GABA neurons, relative to DA neurons, are strongly responsive to aversive events, indicating that they have a broader role in learning.

So far we show, in separate experiments, that DA and GABA neurons respond similarly in rewarding contexts, but that in aversive situations GABA neurons are uniquely recruited. In each of these previous tasks, the learning context was monovalent (appetitive or aversive), and that remained consistent across training. Critically, decision making in natural environments is often multivalent, composed of changing rewards and costs that must be weighed and integrated to guide behavior. Assessing the role of VTA activity in monovalent contexts, as with most previous studies, likely overlooks some of the signaling complexity that must occur when positive and negative variables are simultaneously present and unique computations are required to enable effective decisions.

To reconcile this, we used a motivational conflict task, adapted from our previous studies (Saunders et al., 2013), where rats were required to weigh ongoing,

escalating costs when responding to cues and deciding to engage in reward-seeking behavior. Rats were first trained on the reward conditioning paradigm described above. Next, we introduced an 'aversive barrier' by electrifying the floor bars directly in front of the reward port, while the back of the chamber remained shock free (**Fig. 3A**). The intensity of this constant shock

escalated across sessions, requiring rats to reconcile competing motivations of seeking reward and avoiding footshock. As this 'cost' increased across sessions rats overall decreased their cue-driven reward seeking (**Fig. 3B**). While rats continued overall to consume reward, a smaller proportion of port entries were made during the CS+ period (**Fig. 3C**), and rats on average stayed
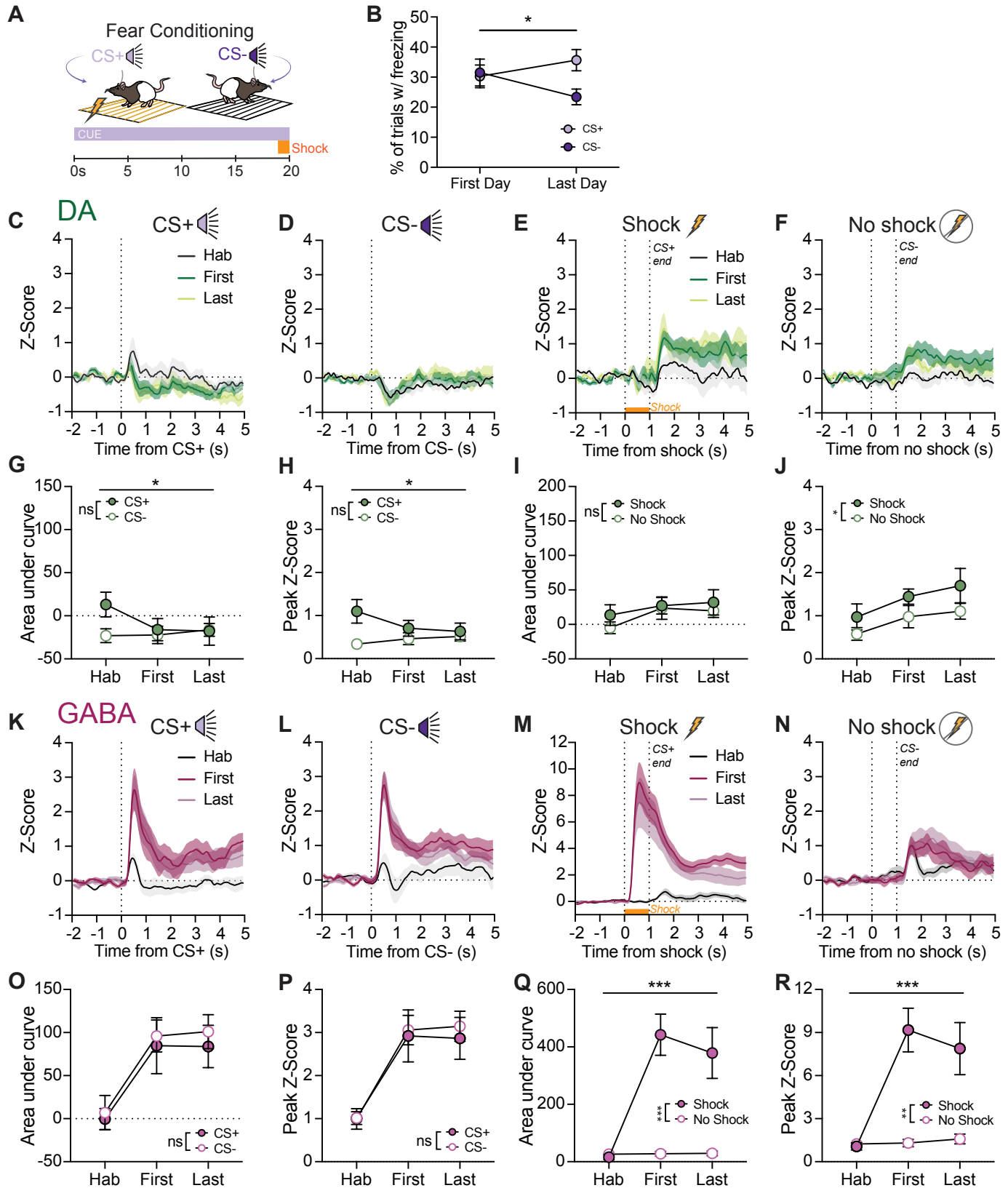
Fig 2 | Conditioned and unconditioned aversive events are strongly encoded by VTA GABA, but not VTA DA neurons

A) Schematic of fear conditioning design. Rats received cue (CS+) + shock (0.4mA, 1s) pairings and a distinct cue (CS-) with no paired outcome, while we recorded GCaMP signals with fiber photometry. **B)** By the end of conditioning, rats learned to discriminate the CS+/CS- cues, as measured by % of trials with a freezing response (two-way ANOVA, cue-type x session interaction $F_{(1,28)}$ = 4.943, P=0.0344). **C-J)** Calcium recordings from VTA DA neurons (n=9). **C)** DA neurons showed minimal responses to the onset of the CS+ and **D)** CS- cues across cue habituation and fear conditioning phases. **E)** There was no DA neuron activity in response to shock itself, and small increases to the offset of the CS+/shock and **F)** offset of the CS- cue. **G)** Across conditioning, DA neuron activity did not discriminate CS+/CS- cues as measured by AUC (two-way repeated measures ANOVA: phase by cue type interaction, $F_{(1.67,13.33)}$=5.55, p=.022; main effect of cue type, $F_{(1,8)}$=2.07, p=.189) and **H)** peak (session by cue interaction, $F_{(1.7,13.7)}$=5.32, p=.023; main effect of cue, $F_{(1,8)}$=5.03, p=.055) measures of the GCaMP signal. **I)** DA neuron activity did not discriminate between the shock period and "no shock" periods corresponding to the end of the CS+ and CS- cues, based on AUC (effect of shock condition, $F_{(1,8)}$=1.32, p=.283). **J)** DA neuron activity at shock offset and CS- offset did increase slightly across conditioning (main effect of phase, $F_{(1.65,13.2)}$=6.76, p=.012), and the peak of this shock offset signal was larger than the CS- offset peak (effect of shock condition, $F_{(1,8)}$=7.77, p=.024). **K-R)** Calcium recordings from VTA GABA neurons (n=13). **K)** GABA neurons developed strong responses to the onset of the CS+ and the **L)** CS- cues between the habituation and conditioning phases. **M)** Shock evoked large, consistent GABA neuron responses, and **N)** the offset of the CS- cue evoked small increases in activity across conditioning. **O)** Strong GABA neuron activity developed to both cues as conditioning progressed, and did not discriminate CS+/CS- according to AUC (effect of phase, $F_{(1.81,21.68)}$=19.45, p<.0001; effect of cue type, $F_{(1,12)}$=1.25, p=.285) and **P)** peak (effect of phase, $F_{(1.88,22.55)}$=20.70, p<.0001; effect of cue type, $F_{(1,12)}$=.229, p=.641) signal measures. **Q)** Robust GABA activity was evoked by shock, relative to the comparable period of time at the end of the CS- cue, based on AUC (phase by shock condition interaction, $F_{(1.85,19.39)}$=14.17, p<.0001), effect of shock condition, $F_{(1,12)}$=27.35, p<.0001) and **R)** peak (phase by shock condition interaction, $F_{(1.84,22.1)}$=11.05, p<.0001), effect of shock condition, $F_{(1,12)}$=18.33, p<.0001) measures. Data reflect subject means +/- SEM. *p< 0.05, **p≤ 0.01, ***p≤ 0.001, ****p≤ 0.0001.

farther away from the reward port (**Fig. 3D**). DA neuron activity to the CS+ weakened as the cue drove less reward-seeking behavior in response to growing cost (**Fig. 3E, I, J**). DA activity to the reward itself or to unrewarded PEs, however, did not change in response to seeking under increasing shock intensity (**Fig. 3G, H, K, L**). GABA neuron activity also decreased on average to the CS+ as the cost escalated and reward seeking became less tied to the cue (**Fig. 3M, Q, R**). Strikingly, in contrast to DA neurons, we found that the GABA reward signal escalated with rising costs. GABA activity was greater to rewarded PEs at higher levels of shock than to rewarded PEs made during sessions of medium and no shock (**Fig. 3O, S, T**). In control studies, we determined that these GABA signals do not simply represent changing perceptual salience, as different intensities of unexpected reward or shock did not evoke different levels of GABA neuron activity (**Supplemental Fig. 3**). This indicates that GABA scaling in our conflict task reflects a state of conditioned motivational salience, rather than a simple readout of stimulus intensity. In the conflict task, we separately analyzed CS+-evoked calcium signals on trials where rats either engaged in a reward seeking response (approach and port entry) during the cue, or did not. We found that cue-evoked GABA, but not DA neuron activity, scaled with motivational state. GABA signals in response to the cue were greater on trials when rats subsequently entered the shock zone to make a reward seeking response (**Fig. 3U-X**). These results indicate that VTA GABA neurons perform a unique computation during reward seeking, compared to DA neurons, encoding motivation as the antecedent cost to seeking rises, and to signal rewarded outcomes experienced under threat.

Taken together, our results motivate an overall re-evaluation of VTA functional heterogeneity, suggesting that DA's contribution to appetitive motivation is potentially collaborative with GABA neuron signaling, which integrates valence to promote motivation in multivalent decision-making states. Our results indicate that GABA neurons reflect a broader learning signal that may direct appropriate behavioral responses in complex environments. Notably, GABA neurons discriminated between the outcome-predictive cue and the neutral cue in the appetitive context but not the aversive context. This suggests that VTA GABA neurons may have a prepotent bias towards threat encoding, which could prime these neurons to integrate negative valence into reward contexts. This conclusion helps consolidate past findings that show evidence for both an "anti-reward" function and an essential reward prediction calculation in VTA GABA neurons (Eshel et al., 2015; Tan et al., 2012).

We found that VTA GABA neuron activity encoded cost in two ways: by scaling responses to reward with escalating cost, and through increased cue-evoked activity on trials where rats seek reward under cost. These results collectively suggest that VTA GABA neurons are important for marshaling reward-seeking motivation and signaling the outcome of actions made under decision conflict. Surprisingly, we find that DA neurons were relatively insensitive to threat or cost, with minimal changes in outcome encoding, and no clear connection between cue-evoked signals and the choice to encounter cost. A relative lack of aversion-mediated calculations recontextualizes previous notions of DA neuron signaling, emphasizing their bias
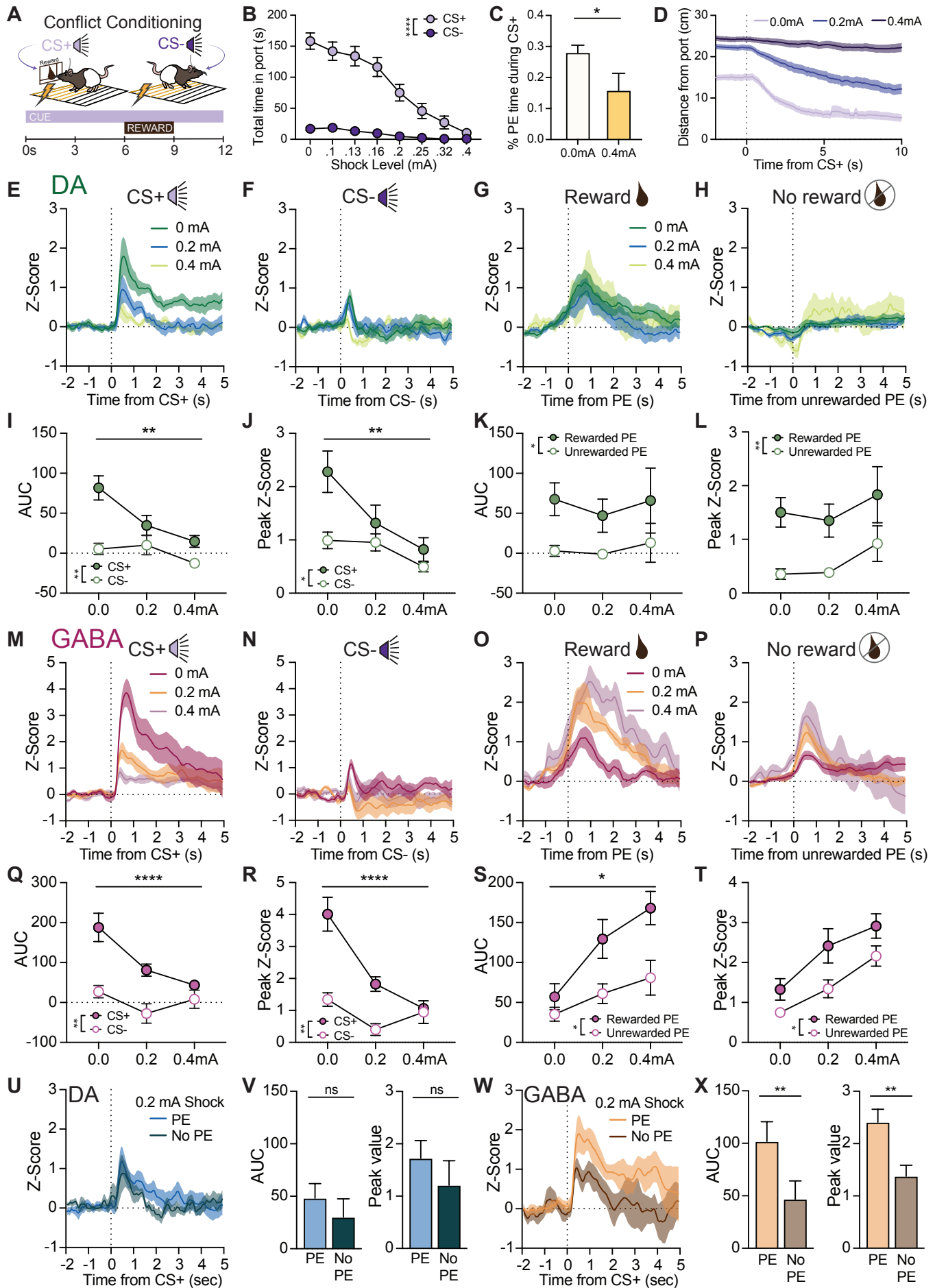
Fig 3 | VTA GABA but not DA neurons integrate valence to encode reward seeking in the face of scaling cost

A) Schematic of experimental design. Rats (N=18) received cue (CS+) + reward (Ensure) pairings and a neutral cue (CS-). After an initial baseline session (0 mA), a cost to reward seeking was introduced in the form of an aversive "barrier". The floor bars in front of the reward port were continuously electrified and shock intensity was gradually escalated across successive sessions. Reward consumption thus required experiencing footshock. **B)** This resulted in a reduction in reward seeking during CS+ presentations (two-way ANOVA, session main effect, $F_{(2.667, 90.69)}=61.03$, P<0.0001; interaction $F_{(7,238)}=37.35$, P<0.0001). **C)** The proportion of time spent in the reward port during the CS+ decreased with cost (paired t test, $t_{(14)}=2.54$, p=.024), although rats continued to make select port entries and consume rewards. **D)** Analysis of approach behavior showed that rats were less likely to rapidly enter the shock zone in response to the cue at higher shock levels. **E-L)** Calcium recordings from VTA DA neurons (n=11). **E)** DA neurons had large CS+ evoked responses initially which reduced as cost increased, **F)** while showing minimal, consistent responses to the CS- cue across cost phase. **G)** Reward consumption evoked consistent DA neuron activity across cost phases, **H)** while unrewarded port entries (PEs) were associated with minimal DA activity. **I)** DA neuron discrimination of CS+/CS- cues decreased as cost escalated, as measured by AUC (two-way repeated measures ANOVA: cost phase by cue interaction, $F_{(1.86,18.58)}=6.71$, p=.0073; main effect of phase, $F_{(1.66,16.64)}=10.75$, p=.0017) and **J)** peak (phase by cue interaction, $F_{(1.61,16.1)}=8.345$, p=.0049; main effect of phase, $F_{(1.55,15.5)}=16.11$, p=.0003) measures of the GCaMP signal. **K)** DA neuron activity discriminated rewarded versus unrewarded PEs but there was no change in the pattern of signal as cost escalated for AUC (phase by response type interaction, $F_{(1.1,8.27)}=.130$, p=.551; effect of response type, $F_{(1,10)}=6.55$, p=.028) or **L)** peak (phase by response type interaction, $F_{(2,15)}=.124$, p=.88; effect of response type, $F_{(1,10)}=11.17$, p=.008) signal measures. **M-T)** Calcium recordings from VTA GABA neurons (n=7). **M)** GABA neurons had large CS+ evoked responses initially which reduced as cost increased, **N)** while showing small, consistent responses to the CS- cue across cost phase. **O)** GABA neuron activity evoked by reward consumption increased as cost escalated, as did **P)** activity in response to unrewarded PEs. **Q)** Average GABA neuron discrimination of CS+/CS- cues decreased as cost escalated, as measured by AUC (two-way repeated measures ANOVA: phase by cue interaction, $F_{(1.73,10.38)}=34.01$, p<.0001; effect of phase, $F_{(1.4,8.38)}=9.202$, p=.01) and **R)** peak (phase by cue interaction, $F_{(1.86,11.17)}=30.97$, p<.0001; main effect of phase, $F_{(1.48,8.9)}=14.82$, p=.0023) measures of the GCaMP signal. **S)** GABA neuron activity discriminated rewarded versus unrewarded PEs, but these signals increased as cost escalated for AUC (phase by response type interaction, $F_{(1.13,4.51)}=9.48$, p=.03; effect of phase, $F_{(1.37,8.24)}=16.06$, p=.0024) and **T)** peak (phase by response type interaction, $F_{(1.38,5.52)}=2.195$, p=.198; effect of phase, $F_{(1.5,9.06)}=22.22$, p=.0005) signal measures. **U-X)** We next examined cue-evoked signals separately on trials where a port entry response did or did not occur, focusing on the 0.2 mA cost session. **U-V)** CS+-evoked DA neuron activity did not discriminate reward seeking under cost (paired t-tests; AUC $t_{(8)}=1.009$, p=.343, peak $t_{(8)}=1.82$, p=.106). **W-X)** In contrast, GABA neuron activity evoked by the CS+ was higher on trials where a PE was made (paired t-tests; AUC $t_{(5)}=5.39$, p=.003, peak $t_{(5)}=4.34$, p=.0074). Data reflect subject means +/- SEM. *p< 0.05, **p≤ 0.01, ****p≤ 0.0001.

to be engaged in monovalent appetitive contexts.

In contrast to previous findings showing that VTA GABA activation results in acute VTA DA inhibition (Tan et al., 2012), our results show that these two populations, recorded from the same area of the VTA, can be active at the same time. Further work is needed to understand this, as complexity of VTA microcircuitry is particularly reflected in GABA neurons, which encompasses local and distal projections that modulate DA through direct inhibition, polysynaptic disinhibition, and amplification of phasic firing (Bocklisch et al., 2013; Lobb et al., 2010; Morozova et al., 2016; Ostroumov et al., 2016; Stamatakis et al., 2013; Tan et al., 2012; Tolu et al., 2013). Further, VTA GABA neurons have several non-DA projection targets outside of the VTA, with unique functional relevance (Al-Hasani et al., 2021; Breton et al., 2019; Oriol et al., 2024; Zhou et al., 2022). Our findings further highlight these complexities, showing important roles for VTA GABA beyond inhibition of DA neurons.

Our results underscore other emerging questions surrounding VTA heterogeneity. We used common markers to target our populations of interest, but there is rich genetic heterogeneity within VTA DA and GABA populations (Miranda-Barrientos et al., 2021; Morales

& Margolis, 2017; Olson & Nestler, 2007; Paul et al., 2019). In comparison studies, VTA calcium recordings using another GABAergic marker, mDlx, also showed similar appetitive and aversive encoding (Supplemental Fig. 4), indicating that this activity phenotype is not specific to Gad1 neurons. Functional heterogeneity among different GABA populations remains a relatively open area of investigation (Koutlas et al., 2024; Margolis et al., 2012; Root et al., 2020; Wang et al., 2024). It remains unclear, for example, if there are distinct VTA GABA ensembles that preferentially respond to positive valence or negative valence, and/or uniquely engage local DA neurons.

Our results indicate that VTA GABA neurons have a much more active role in conditioned appetitive motivation than previously appreciated. Given the prominence of multi-valent contexts in natural decision making, the pattern we describe for VTA GABA neurons may be a standard encoding profile, rather than the exception. These data point to the need for a strong experimental focus on VTA heterogeneity in complex learning and decision-making frameworks, as well as compulsive disease models.

METHODS

Subjects: Male and female Long Evans rats were used (N=34; 13F, 21M). Dopamine neurons were targeted in TH-cre transgenic rats, expressing Cre recombinase under the tyrosine hydroxylase (TH) promoter (Engel et al., 2024; Witten et al., 2011). GABA neurons were targeted in wild type rats. All rats weighed 250-600g at the time of surgery and were 3-6 months old at the time of behavior and photometry recordings. Rats were paired or singly housed throughout the duration of the experiment in a vivarium with a 12-hour light / 12-hour dark cycle (lights on at 0700, lights off at 1900) with *ad libitum* access to food and water. During the reward conditioning and motivational conflict phase animals were food restricted - fed once/day to maintain 90% free feeding body weight. All procedures involving animal subjects were in compliance with Institutional Animal Care and Use Committee (IACUC) approval and in accordance with the National Institutes of Health's animal care guidelines.

Viral vectors: To target dopamine neurons, a cre-dependent AAV coding for GCaMP8f was injected into the VTA in TH-cre positive rats (750nL, AAV5-syn-DIO-jGCaMP8f-WPRE; Addgene). To target GABA neurons generally, an AAV delivering Cre under the Gad1 promoter (AAV5-Gad1-cre; University of Minnesota Viral Vector and Cloning Core) was simultaneously infused with the cre-dependent GCaMP8f or GCaMP8m into the VTA of wildtype rats (125-250nL Gad1-Cre, 250-750nL DIO-GCaMP), similar to previous studies (Scott et al., 2023; Wakabayashi et al., 2019). A separate set of wildtype rats received VTA-targeted injections of a GCaMP virus under the GABAergic interneuron promotor mDlx (800nL, AAV5-mDlx-GCaMP6f; Addgene).

Stereotaxic surgery: Rats were induced under 5% isoflurane anesthesia and maintained at 1-3% for the duration of the surgery. Rats received carprofen (5 mg/kg), cefazolin (70 mg/kg), and saline subcutaneously at the beginning of the surgery. An incision was made to reveal the top of the skull and holes were drilled for viral delivery (-5.6 A-P, -/+0.8 M-L, -8.2 D-V), optic fiber placement (-5.6 A-P, -/+0.8 M-L, -8.0 D-V), and skull screws. All coordinates are in mm relative to bregma and skull surface. Viruses were delivered at a rate of 0.1µL/min. Once infusion finished, the needle was raised 100 µm and left to sit for 10 minutes before being fully removed. Optic fiber implants (9mm length, 400µm diameter, Doric Lenses) were lowered into the VTA and secured in place with dental acrylic around the skull screws. Topical anesthetic and antibiotic were applied to the incision area and rat was monitored on a heating pad in a sterile home cage until fully alert and awake. Rats were given carprofen and cefazolin for three days following surgery and weighed with health evaluations for 6 days. Rats recovered for at least 4 weeks following viral injection before beginning experiments.

Fiber photometry recordings: To assess Ca^{2+} dynamics in the VTA during Pavlovian conditioning, we measured GCaMP fluorescence using fiber photometry. For all behavioral experiments, rats were tethered to a low autofluorescence optic cable sheathed in a lightweight armored jacket (Doric-Lenses). Some behavioral sessions did not record photometry signals to avoid photobleaching the GCaMP fluorescent proteins. Recording data included here are sampled from the early (Day 1), middle (Days 8 or 9), and late (Day 13 or 15) of reward conditioning. On photometry recording days, 415 nm and 465 nm LEDs (Doric-Lenses) set at 50µW were delivered via a fluorescence mini-cube (Doric-Lenses). The isosbestic (415) and Ca^{2+} dependent (465) channels were sinusoidally modulated at 211Hz and 330Hz respectively. Fluorescence from the implanted optic fiber was transmitted through the mini-cube to be filtered, amplified, and focused onto a high sensitivity photoreceiver (Newport, Model 2151). A real-time signal processor (RZ5P, Tucker Davis Technologies) using Synapse software modulated the power of the LED output and recorded photometry signals, sampled at 6.1kHz. Events during the behavioral session (e.g., foot shock and cue presentations), were recorded in the photometry data file with a TTL signal time stamp from the MED-PC behavioral program. Videos of each behavioral session were recorded at 10-20 FPS with corresponding timestamps of each frame in the photometry file.

Habituation: Before any behavioral testing, animals were habituated to cable tethering and med-associates chambers with 1-2 habituation sessions of 30 minutes with the chamber lights and fans running.

Reward conditioning: Animals received between 13 and 15 days of reward conditioning. Each session consisted of 20 conditioned stimulus plus (CS+) and 20 conditioned stimulus minus (CS-) presentations. The CS+ and CS- were distinct auditory stimuli counterbalanced across animals. The CS+ was 12 seconds long with the onset of a pump providing Ensure reward delivered between seconds 6 and 9. The CS- was 12 seconds long with no additional events. Reward seeking was measured by duration of time in the reward magazine during the CS+,

CS- or inter-trial interval (ITI).

Fear conditioning: Animals received 3 days of fear conditioning. Each session consisted of 15 conditioned stimulus shock (CS+) and 15 conditioned stimulus minus (CS-) presentations. The CS+ and CS- were distinct auditory stimuli counterbalanced across animals. The CS+ was 20 seconds long with the onset of a 0.4mA footshock delivered during the last second. The CS- was 20 seconds long with no additional events.

Motivational conflict task: Animals received 8 days of the motivational conflict paradigm (Adapted from Saunders et al., 2013). Each session consisted of 20 CS+ and 10 CS- presentations. The cues and the pump were the same as during reward conditioning. On sessions 2-8, the 7 floor bars closest to the reward magazine were electrified with a mild electric shock. The shock ranged from 0.0mA - 0.4mA and increased across the 8 sessions. Reward seeking was measured by duration of time in the reward magazine during the CS+, CS- or inter-trial interval (ITI).

Stimulus scaling - reward: Animals received 30 unexpected rewards equally split between 80% or 20% Ensure diluted with water. 80% and 20% Ensure were delivered on opposite sides of the chamber to the right or left magazine on the first day and swapped for the second day. Photometry traces were time-locked to the first port entry following the pump and averaged across both sessions.

Stimulus scaling - shock: Animals received 5 unexpected foot shocks of 0.2mA and 0.4mA for 1 second each. The order of shock intensities was counterbalanced across animals.

Fiber Photometry Analysis: Recordings were analyzed with a custom MATLAB (Mathworks) pipeline. First, signals were lowpass filtered, downsampled to 40Hz, and a least squares linear fit was applied to the isosbestic channel (415 nm) to align it to the calcium-dependent, 465 nm, channel. The fitted isosbestic channel was then used to normalize the 465 signal with the calculation $\Delta F/F$ = (465-nm signal – fitted 415-nm signal)/(fitted 415-nm signal). Individual trial traces were z-scored to the 5s immediately preceding cue, port entry, and footshock events in order to avoid effects of drift across the session. Area under the curve (AUC) values took the z-scored trace and calculated numerical integration via the trapezoidal method using the trapz function (MATLAB). AUC and peak Z-score values were calculated between event onset and 2 seconds immediately after.

Automated pose-estimation: Markerless tracking of animal body parts was conducted using version 2.2.1.1 of the DeepLabCut (DLC) Toolbox (Mathis et al., 2018) and analysis of movement features based on these tracked coordinates was conducted in MATLAB. DeepLabCut 2.2.1.1 was installed in an Anaconda environment with Python 3.8.4, CUDA 11.7 and Tensorflow 2.10. *DeepLabCut Model:* 2090 frames from 35 videos (32 different animals, 3 experiments) were labeled and 807 outlier frames were re-labelled to refine the network. Labeled frames were split into a training set (95% of frames) and a test set (5% of frames). A ResNet-50 based neural network (Insafutdinov et al., 2016) was used for 1,030,000 training iterations. After the final refinement we found the test error was 4.1 pixels, the training error was 3.13 pixels and with a p-cutoff of 0.85 training error was 2.99 pixels and test error was 3.68 pixels. The body parts labeled included the nose, eyes, ears, center of head or fiber optic implant, shoulders, tail base, and an additional three points along the spine. Features of the environment were also labeled, including the 4 corners of the apparatus floor, two nose ports, two cue lights, two magazine ports, and 3 LED indicator lights when active. DLC coordinates and confidence values for each body part and frame were imported to Matlab and filtered to exclude body parts/features from any frame where the confidence was < 0.7. For labeled features of the environment, which have a fixed location, the average coordinates for that recording were used for analysis. To convert pixel distances to the real chamber dimensions, for each video, a pixel to cm conversion rate was determined. The distance (in pixels) between each edge of the environment floor and the diagonal measurements from corner to corner was measured, and these values were divided by the actual distance in cm. The mean of these values was then used as the conversion factor.

Freezing was detected by assessing locomotion of the nose, implant, left and right ears, and 4 points spanning the length of the animals back. The movement threshold for detecting locomotion was calibrated to animal size using a scale factor determined from the relationship between body size (distance between the shoulder and bottom back point) and the optimal threshold for detecting movement in a separate group of animals not used for this study (n = 4). This threshold was used to detect movements in the face and head, and for remaining body parts this value was multiplied by two to accommodate detection of the finer movements in the face/head vs larger movements in the body. Freezing bouts were detected when all of the visible body parts were below the respective movement threshold and a sliding window (0.3s) was used to determine when the speed of 2 or more body parts exceeded the

movement threshold for the window duration, indicating the beginning and end of a freezing bout. Freezing periods shorter than 1s in duration were excluded and frames in which less than 3 body parts were visible were ignored. The starts and ends of bouts were removed if they consisted only of frames where an insufficient number bodyparts were visible. We quantified freezing as the percent of trials with freezing initiated in the last 5 seconds of the CS+ or CS- prior to the footshock or lack thereof (seconds 14-19 post-cue onset).

Histology: After experiments, rats received i.p. injections of Fatal-Plus (2 ml/kg; Patterson Veterinary) to induce a deep anesthesia and were transcardially perfused with cold phosphate buffered saline (PBS) followed by 4% paraformaldehyde (PFA). Brains were removed and post-fixed in 4% PFA for ~24 h, then cryoprotected in a 25% sucrose in PBS for 48 h or until sectioning. Tissue was sliced at 40 microns on a cryostat (Leica CM1900). To confirm viral expression and optic fiber placements, brain sections containing the midbrain were mounted on microscope slides and coverslipped using Vectashield mounting medium containing DAPI counterstain. Fiber tissue damage was then visualized on a Keyence BZ-X710 microscope. Rats were included in analysis only if fiber damage was no more than 500 microns dorsal to the target regions.

Immunohistochemistry: Sections were washed in PBS and incubated with bovine serum albumin (BSA) and Triton X-100 (each 0.2%) for 20 min. 10% normal donkey serum (NDS) was added for a 30-min incubation, before primary antibody incubation (rabbit anti-TH, 1:500, Fisher Scientific and/or mouse anti-GFP, 1:500, Abcam) overnight at 4 °C in PBS with BSA and Triton X-100 (each 0.2%). Sections were then washed and incubated with 2% NDS in PBS for 10 min and secondary antibody was added (1:200 Alexa Fluor 594 donkey anti-rabbit and/or 1:200 Alexa Fluor 488 donkey anti-mouse) for 2 h at room temperature. Sections were washed twice in PBS, mounted on microscope slides, and coverslipped with Vectashield containing DAPI counterstain.

Statistical analysis: Behavioral and neural activity data were analyzed with a combination of 2-way mixed effects ANOVAs, planned t tests, and Pearson correlations. Post-hoc comparisons were completed with Bonferroni corrections. Summary figures represent averages of subjects with mean ± S.E.M. Statistical significance was set at $p < 0.05$. Photometry and video data were analyzed in MATLAB. Visualization and statistical analyses were performed using Graphpad Prism 10.0.

REFERENCES

Al-Hasani, R., Gowrishankar, R., Schmitz, G. P., Pedersen, C. E., Marcus, D. J., Shirley, S. E., Hobbs, T. E., Elerding, A. J., Renaud, S. J., Jing, M., Li, Y., Alvarez, V. A., Lemos, J. C., & Bruchas, M. R. (2021). Ventral tegmental area GABAergic inhibition of cholinergic interneurons in the ventral nucleus accumbens shell promotes reward reinforcement. Nature Neuroscience, 24(10), Article 10. https://doi.org/10.1038/s41593-021-00898-2

Berke, J. D. (2018). What does dopamine mean? Nature Neuroscience, 21(6), 787–793. https://doi.org/10.1038/s41593-018-0152-y

Bocklisch, C., Pascoli, V., Wong, J. C. Y., House, D. R. C., Yvon, C., de Roo, M., Tan, K. R., & Lüscher, C. (2013). Cocaine Disinhibits Dopamine Neurons by Potentiation of GABA Transmission in the Ventral Tegmental Area. Science, 341(6153), 1521–1525. https://doi.org/10.1126/science.1237059

Bouarab, C., Thompson, B., & Polter, A. M. (2019). VTA GABA Neurons at the Interface of Stress and Reward. Frontiers in Neural Circuits, 13. https://www.frontiersin.org/articles/10.3389/fncir.2019.00078

Breton, J. M., Charbit, A. R., Snyder, B. J., Fong, P. T. K., Dias, E. V., Himmels, P., Lock, H., & Margolis, E. B. (2019). Relative contributions and mapping of ventral tegmental area dopamine and GABA neurons by projection target in the rat. Journal of Comparative Neurology, 527(5), 916–941. https://doi.org/10.1002/cne.24572

Brischoux, F., Chakraborty, S., Brierley, D. I., & Ungless, M. A. (2009). Phasic excitation of dopamine neurons in ventral VTA by noxious stimuli. Proceedings of the National Academy of Sciences, 106(12), 4894–4899. https://doi.org/10.1073/pnas.0811507106

Cai, L. X., Pizano, K., Gundersen, G. W., Hayes, C. L., Fleming, W. T., Holt, S., Cox, J. M., & Witten, I. B. (2020). Distinct signals in medial and lateral VTA dopamine neurons modulate fear extinction at different times. eLife, 9, e54936. https://doi.org/10.7554/eLife.54936

Cohen, J. Y., Haesler, S., Vong, L., Lowell, B. B., & Uchida, N. (2012). Neuron-type-specific signals for reward and punishment in the ventral tegmental area. Nature, 482(7383), Article 7383. https://doi.org/10.1038/nature10754

Cox, J., & Witten, I. B. (2019). Striatal circuits for reward learning and decision-making. Nature Reviews Neuroscience, 20(8), Article 8. https://doi.org/10.1038/s41583-019-0189-2

Day, J. J., Roitman, M. F., Wightman, R. M., & Carelli, R. M. (2007). Associative learning mediates dynamic shifts in dopamine signaling in the nucleus accumbens. Nature Neuroscience, 10(8), Article 8. https://doi.org/10.1038/nn1923

Engel, L., Wolff, A. R., Blake, M., Collins, V. L., Sinha, S., & Saunders, B. T. (2024). Dopamine neurons drive spatiotemporally heterogeneous striatal dopamine signals during learning. Current Biology: CB, 34(14), 3086-3101.e4. https://doi.org/10.1016/j.cub.2024.05.069

Eshel, N., Bukwich, M., Rao, V., Hemmelder, V., Tian, J., & Uchida, N. (2015). Arithmetic and local circuitry underlying dopamine prediction errors. Nature, 525(7568), Article 7568. https://doi.org/10.1038/nature14855

Howe, M. W., & Dombeck, D. A. (2016). Rapid signalling in distinct dopaminergic axons during locomotion and reward. Nature, 535(7613), 505–510. https://doi.org/10.1038/nature18942

Hughes, R. N., Watson, G. D. R., Petter, E. A., Kim, N., Bakhurin, K. I., & Yin, H. H. (2019). Precise Coordination of Three-dimensional Rotational Kinematics by Ventral Tegmental Area GABAergic Neurons. Current Biology : CB, 29(19), 3244-3255.e4. https://doi.org/10.1016/j.cub.2019.08.022

Insafutdinov, E., Pishchulin, L., Andres, B., Andriluka, M., & Schiele, B. (2016). DeeperCut: A Deeper, Stronger, and Faster Multi-Person Pose Estimation Model (No. arXiv:1605.03170). arXiv. http://arxiv.org/abs/1605.03170

Jo, Y. S., Heymann, G., & Zweifel, L. S. (2018). Dopamine Neurons Reflect the Uncertainty in Fear Generalization. Neuron, 100(4), 916-925.e3. https://doi.org/10.1016/j.neuron.2018.09.028

Keiflin, R., & Janak, P. H. (2015). Dopamine Prediction Errors in Reward Learning and Addiction: From Theory to Neural Circuitry. Neuron, 88(2), 247–263. https://doi.org/10.1016/j.neuron.2015.08.037

Keiflin, R., Pribut, H. J., Shah, N. B., & Janak, P. H. (2019). Ventral Tegmental Dopamine Neurons Participate in Reward Identity Predictions. Current Biology, 29(1), 93-103.e3. https://doi.org/10.1016/j.cub.2018.11.050

Kim, Y.-B., Matthews, M., & Moghaddam, B. (2010). Putative γ-aminobutyric acid neurons in the ventral tegmental area have a similar pattern of plasticity as dopamine neurons during appetitive and aversive learning. European Journal of Neuroscience, 32(9), 1564–1572. https://doi.org/10.1111/j.1460-9568.2010.07371.x

Koutlas, I., Patrikiou, L., Van Der Starre, S. E., Danko, D., Wolterink-Donselaar, I. G., Luijendijk, M. C. M., Adan, R. A. H., & Meye, F. J. (2024). Distinct ventral tegmental area neuronal ensembles are indispensable for reward-driven approach and stress-driven avoidance behaviors. https://doi.org/10.1101/2024.05.30.596611

Lefner, M. J., & Moghaddam, B. (2024). Reward and punishment contingency shifting reveals distinct roles for VTA dopamine and GABA neurons in behavioral flexibility (p. 2024.10.07.617060). bioRxiv. https://doi.org/10.1101/2024.10.07.617060

Lobb, C. J., Wilson, C. J., & Paladini, C. A. (2010). A Dynamic Role for GABA Receptors on the Firing Pattern of Midbrain Dopaminergic Neurons. Journal of Neurophysiology, 104(1), 403–413. https://doi.org/10.1152/jn.00204.2010

Margolis, E. B., Toy, B., Himmels, P., Morales, M., & Fields, H. L. (2012). Identification of Rat Ventral Tegmental Area GABAergic Neurons. PLOS ONE, 7(7), e42365. https://doi.org/10.1371/journal.pone.0042365

Mathis, A., Mamidanna, P., Cury, K. M., Abe, T., Murthy, V. N., Mathis, M. W., & Bethge, M. (2018). DeepLabCut: Markerless pose estimation of user-defined body parts with deep learning. Nature Neuroscience, 21(9), Article 9. https://doi.org/10.1038/s41593-018-0209-y

Miranda-Barrientos, J., Chambers, I., Mongia, S., Liu, B., Wang, H.-L., Mateo-Semidey, G. E., Margolis, E. B., Zhang, S., & Morales, M. (2021). Ventral tegmental area GABA, glutamate, and glutamate-GABA neurons are heterogeneous in their electrophysiological and pharmacological properties. European Journal of Neuroscience, 54(1), 4061–4084. https://doi.org/10.1111/ejn.15156

Morales, M., & Margolis, E. B. (2017). Ventral tegmental area: Cellular heterogeneity, connectivity and behaviour. Nature Reviews Neuroscience, 18(2), Article 2. https://doi.org/10.1038/nrn.2016.165

Morozova, E. O., Myroshnychenko, M., Zakharov, D., di Volo, M., Gutkin, B., Lapish, C. C., & Kuznetsov, A. (2016). Contribution of synchronized GABAergic neurons to dopaminergic neuron firing and bursting. Journal of Neurophysiology, 116(4), 1900–1923. https://doi.org/10.1152/jn.00232.2016

Nair-Roberts, R. G., Chatelain-Badie, S. D., Benson, E., White-Cooper, H., Bolam, J. P., & Ungless, M. A. (2008). Stereological estimates of dopaminergic, GABAergic and glutamatergic neurons in the ventral tegmental area, substantia nigra and retrorubral field in the rat. Neuroscience, 152(4), 1024–1031. https://doi.org/10.1016/j.neuroscience.2008.01.046

Olson, V. G., & Nestler, E. J. (2007). Topographical organization of GABAergic neurons within the ventral tegmental area of the rat. Synapse, 61(2), 87–95. https://doi.org/10.1002/syn.20345

Oriol, L., Chao, M., Kollman, G. J., Dowlat, D. S., Singhal, S. M., Steinkellner, T., & Hnasko, T. S. (2024). Ventral tegmental area interneurons revisited: GABA and glutamate projection neurons make local synapses. eLife, 13. https://doi.org/10.7554/eLife.100085.1

Ostroumov, A., Thomas, A. M., Kimmey, B. A., Karsch, J. S., Doyon, W. M., & Dani, J. A. (2016). Stress Increases Ethanol Self-Administration via a Shift toward Excitatory GABA Signaling in the Ventral Tegmental Area. Neuron, 92(2), 493–504. https://doi.org/10.1016/j.neuron.2016.09.029

Park, J., & Moghaddam, B. (2017). Risk of punishment influences discrete and coordinated encoding of reward-guided actions by prefrontal cortex and VTA neurons. eLife, 6, e30056. https://doi.org/10.7554/eLife.30056

Paul, E. J., Tossell, K., & Ungless, M. A. (2019). Transcriptional profiling aligned with in situ expression image analysis reveals mosaically expressed molecular markers for GABA neuron sub-groups in the ventral tegmental area. European Journal of Neuroscience, 50(11), 3732–3749. https://doi.org/10.1111/ejn.14534

Root, D. H., Barker, D. J., Estrin, D. J., Miranda-Barrientos,

J. A., Liu, B., Zhang, S., Wang, H.-L., Vautier, F., Ramakrishnan, C., Kim, Y. S., Fenno, L., Deisseroth, K., & Morales, M. (2020). Distinct Signaling by Ventral Tegmental Area Glutamate, GABA, and Combinatorial Glutamate-GABA Neurons in Motivated Behavior. Cell Reports, 32(9), 108094. https://doi.org/10.1016/j.celrep.2020.108094

Saunders, B. T., Richard, J. M., Margolis, E. B., & Janak, P. H. (2018). Dopamine neurons create Pavlovian conditioned stimuli with circuit-defined motivational properties. Nature Neuroscience, 21(8), Article 8. https://doi.org/10.1038/s41593-018-0191-4

Saunders, B. T., Yager, L. M., & Robinson, T. E. (2013). Cue-Evoked Cocaine "Craving": Role of Dopamine in the Accumbens Core. Journal of Neuroscience, 33(35), 13989–14000. https://doi.org/10.1523/JNEUROSCI.0450-13.2013

Schultz, W. (2006). Behavioral theories and the neurophysiology of reward. Annual Review of Psychology, 57, 87–115. https://doi.org/10.1146/annurev.psych.56.091103.070229

Schultz, W. (2016). Dopamine reward prediction-error signalling: A two-component response. Nature Reviews Neuroscience, 17(3), 183–195. https://doi.org/10.1038/nrn.2015.26

Schultz, W., Dayan, P., & Montague, P. R. (1997). A Neural Substrate of Prediction and Reward. Science, 275(5306), 1593–1599. https://doi.org/10.1126/science.275.5306.1593

Scott, A., Palmer, D., Newell, B., Lin, I., Cayton, C. A., Paulson, A., Remde, P., & Richard, J. M. (2023). Ventral Pallidal GABAergic Neuron Calcium Activity Encodes Cue-Driven Reward Seeking and Persists in the Absence of Reward Delivery. The Journal of Neuroscience: The Official Journal of the Society for Neuroscience, 43(28), 5191–5203. https://doi.org/10.1523/JNEUROSCI.0013-23.2023

Sharpe, M. J., Chang, C. Y., Liu, M. A., Batchelor, H. M., Mueller, L. E., Jones, J. L., Niv, Y., & Schoenbaum, G. (2017). Dopamine transients are sufficient and necessary for acquisition of model-based associations. Nature Neuroscience, 20(5), 735–742. https://doi.org/10.1038/nn.4538

Stamatakis, A. M., Jennings, J. H., Ung, R. L., Blair, G. A., Weinberg, R. J., Neve, R. L., Boyce, F., Mattis, J., Ramakrishnan, C., Deisseroth, K., & Stuber, G. D. (2013). A Unique Population of Ventral Tegmental Area Neurons Inhibits the Lateral Habenula to Promote Reward. Neuron, 80(4), 1039–1053. https://doi.org/10.1016/j.neuron.2013.08.023

Steinberg, E. E., Keiflin, R., Boivin, J. R., Witten, I. B., Deisseroth, K., & Janak, P. H. (2013). A causal link between prediction errors, dopamine neurons and learning. Nature Neuroscience, 16(7), Article 7. https://doi.org/10.1038/nn.3413

Swanson, L. W. (1982). The projections of the ventral tegmental area and adjacent regions: A combined fluorescent retrograde tracer and immunofluorescence study in the rat. Brain Research Bulletin, 9(1–6), 321–353. https://doi.org/10.1016/0361-9230(82)90145-9

Tan, K. R., Yvon, C., Turiault, M., Mirzabekov, J. J., Doehner, J., Labouèbe, G., Deisseroth, K., Tye, K. M., & Lüscher, C.

(2012). GABA Neurons of the VTA Drive Conditioned Place Aversion. Neuron, 73(6), 1173–1183. https://doi.org/10.1016/j.neuron.2012.02.015

Taylor, S. R., Badurek, S., Dileone, R. J., Nashmi, R., Minichiello, L., & Picciotto, M. R. (2014). GABAergic and glutamatergic efferents of the mouse ventral tegmental area. Journal of Comparative Neurology, 522(14), 3308–3334. https://doi.org/10.1002/cne.23603

Tolu, S., Eddine, R., Marti, F., David, V., Graupner, M., Pons, S., Baudonnat, M., Husson, M., Besson, M., Reperant, C., Zemdegs, J., Pagès, C., Hay, Y. a. H., Lambolez, B., Caboche, J., Gutkin, B., Gardier, A. M., Changeux, J.-P., Faure, P., & Maskos, U. (2013). Co-activation of VTA DA and GABA neurons mediates nicotine reinforcement. Molecular Psychiatry, 18(3), 382–393. https://doi.org/10.1038/mp.2012.83

Tsai, H.-C., Zhang, F., Adamantidis, A., Stuber, G. D., Bonci, A., de Lecea, L., & Deisseroth, K. (2009). Phasic Firing in Dopaminergic Neurons Is Sufficient for Behavioral Conditioning. Science, 324(5930), 1080–1084. https://doi.org/10.1126/science.1168878

van Zessen, R., Phillips, J. L., Budygin, E. A., & Stuber, G. D. (2012). Activation of VTA GABA Neurons Disrupts Reward Consumption. Neuron, 73(6), 1184–1194. https://doi.org/10.1016/j.neuron.2012.02.016

Wakabayashi, K. T., Feja, M., Baindur, A. N., Bruno, M. J., Bhimani, R. V., Park, J., Hausknecht, K., Shen, R.-Y., Haj-Dahmane, S., & Bass, C. E. (2019). Chemogenetic activation of ventral tegmental area GABA neurons, but not mesoaccumbal GABA terminals, disrupts responding to reward-predictive cues. Neuropsychopharmacology: Official Publication of the American College of Neuropsychopharmacology, 44(2), 372–380. https://doi.org/10.1038/s41386-018-0097-6

Wang, F., Liu, C., Wang, Y., Wang, X., Yang, Y., Jiang, C., Le, Q., Liu, X., Ma, L., & Wang, F. (2024). Morphine- and foot shock-responsive neuronal ensembles in the VTA possess different connectivity and biased GPCR signaling pathway. Theranostics, 14(3), 1126–1146. https://doi.org/10.7150/thno.90792

Witten, I. B., Steinberg, E. E., Lee, S. Y., Davidson, T. J., Zalocusky, K. A., Brodsky, M., Yizhar, O., Cho, S. L., Gong, S., Ramakrishnan, C., Stuber, G. D., Tye, K. M., Janak, P. H., & Deisseroth, K. (2011). Recombinase-Driver Rat Lines: Tools, Techniques, and Optogenetic Application to Dopamine-Mediated Reinforcement. Neuron, 72(5), 721–733. https://doi.org/10.1016/j.neuron.2011.10.028

Zhou, W.-L., Kim, K., Ali, F., Pittenger, S. T., Calarco, C. A., Mineur, Y. S., Ramakrishnan, C., Deisseroth, K., Kwan, A. C., & Picciotto, M. R. (2022). Activity of a direct VTA to ventral pallidum GABA pathway encodes unconditioned reward value and sustains motivation for reward. Science Advances, 8(42), eabm5217. https://doi.org/10.1126/sciadv.abm5217
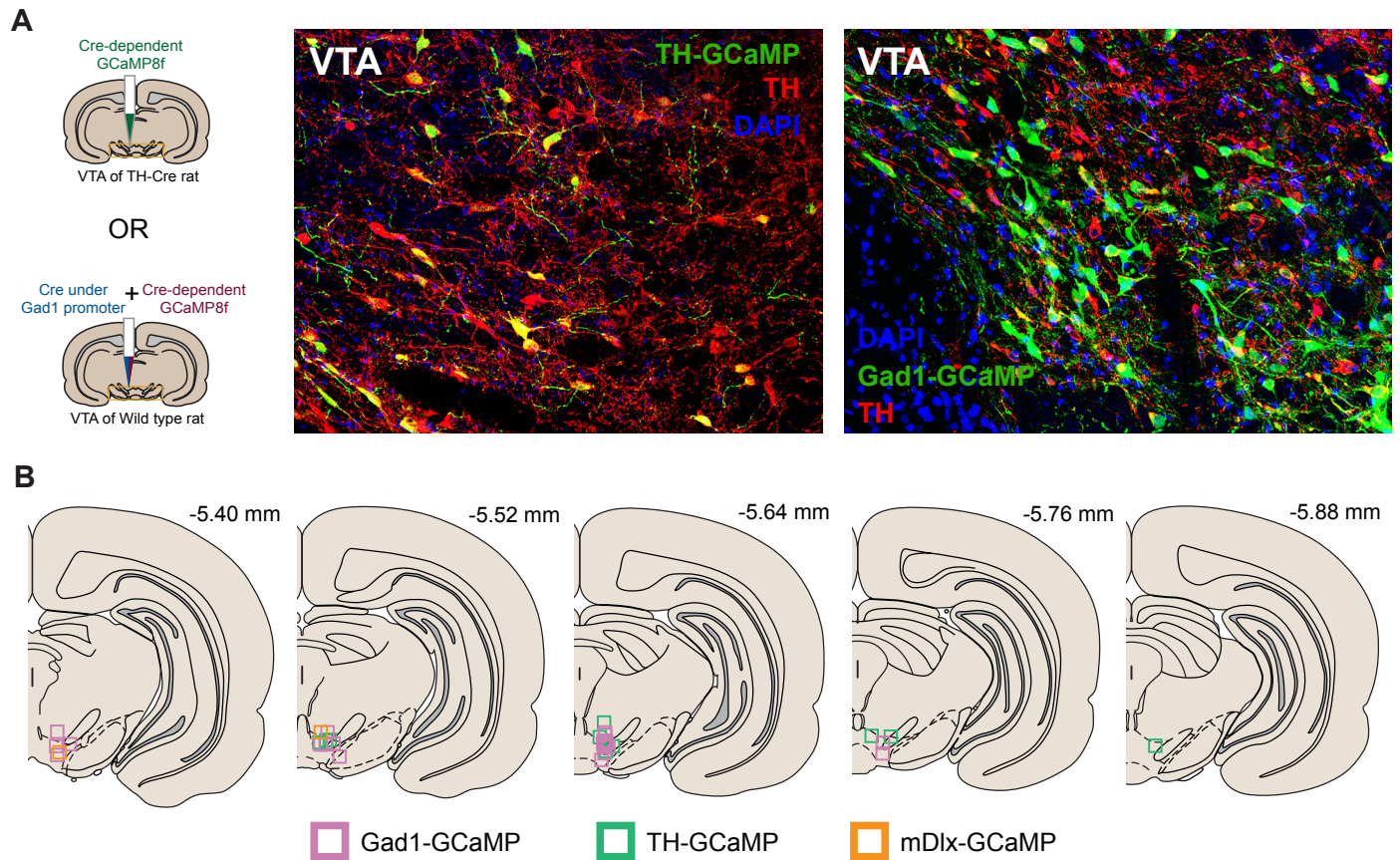
Supplemental Fig 1 | Histology and fiber placements in the VTA for GABA and DA targeted GCaMP recordings

A) Example histological targeting. TH+ neurons were targeted with a cre-dependent AAV in TH-cre rats, with good specificity. Using a dual-virus approach, GAD1+ neurons were targeted, resulting in minimal expression in TH+ neurons in the VTA. B) Optic fiber placements for rats in recording experiments. Pink squares represent Gad1-targeted rats. Green squares represent TH-targeted rats. Orange squares represent mDlx-targeted rats.
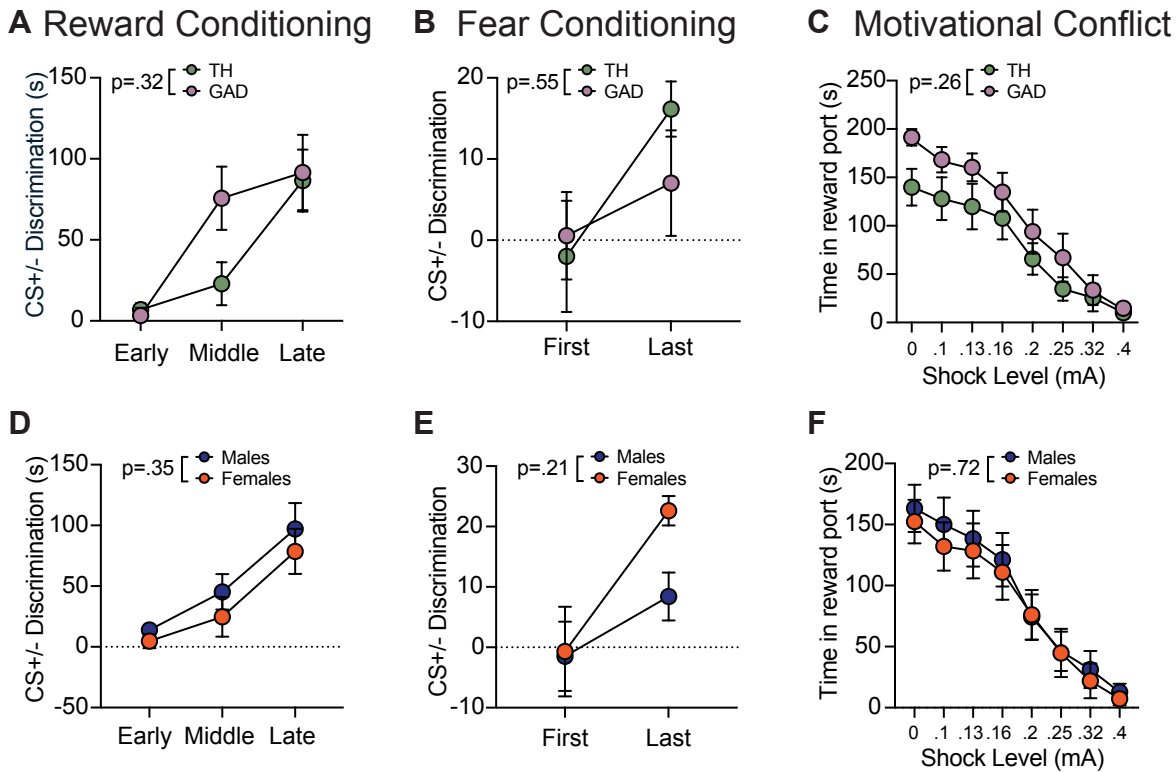
Supplemental Fig 2 | Conditioned behavior did not significantly differ across cohorts

A) Gad and TH animals achieved the same level of cue discrimination during reward conditioning as measured by the difference in reward port duration between the CS+ and the CS-, indicating comparable learning. **B)** Gad and TH animals achieved the same level of discrimination during fear conditioning as measured by the difference in percent trials with freezing between the CS+ and the CS-. **C)** Gad and TH animals similarly decreased their cued responding during motivational conflict as shock intensity escalated, as measured by seconds in the reward port. **D)** Male and female animals achieved the same level of discrimination during reward conditioning as measured by the difference in reward port duration between the CS+ and the CS-. **E)** Male and female animals achieved the same level of discrimination during fear conditioning as measured by the difference in percent trials with freezing between the CS+ and the CS-. **F)** Male and female animals decreased responding similarly during motivational conflict as shock intensity escalated, as measured by seconds in the reward port.
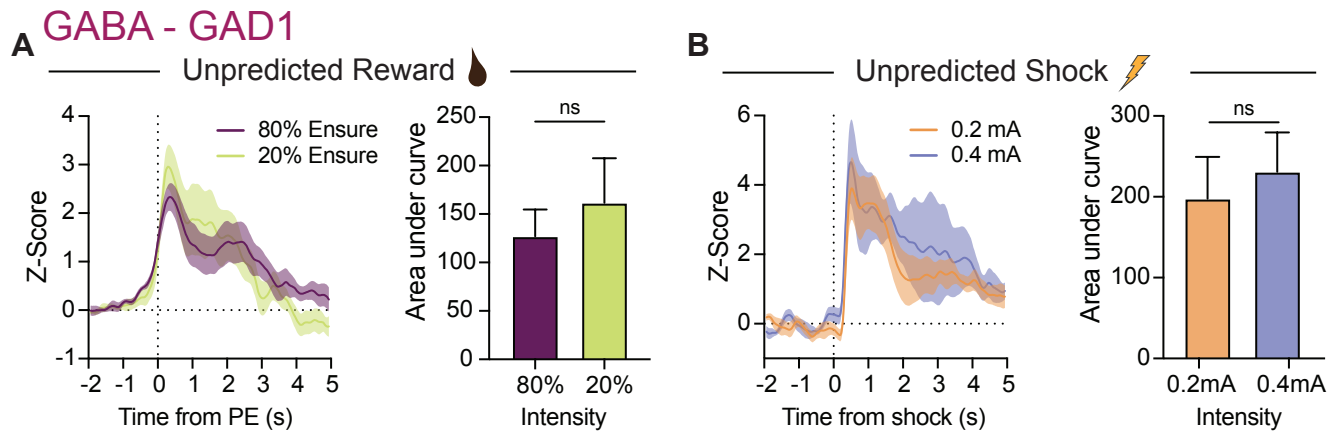
Supplemental Fig 3 | VTA GABA neuron activity does not reliably scale with stimulus intensity

A) Reward consumption evoked similar VTA GABA neuron activity regardless of concentration as measured by AUC (paired t test, $t(6)=1.18$, $p=.281$). **B)** Footshock evoked similar VTA GABA neuron activity regardless of electrical charge as measured by AUC (paired t test, $t(6)=0.65$, $p=.542$).
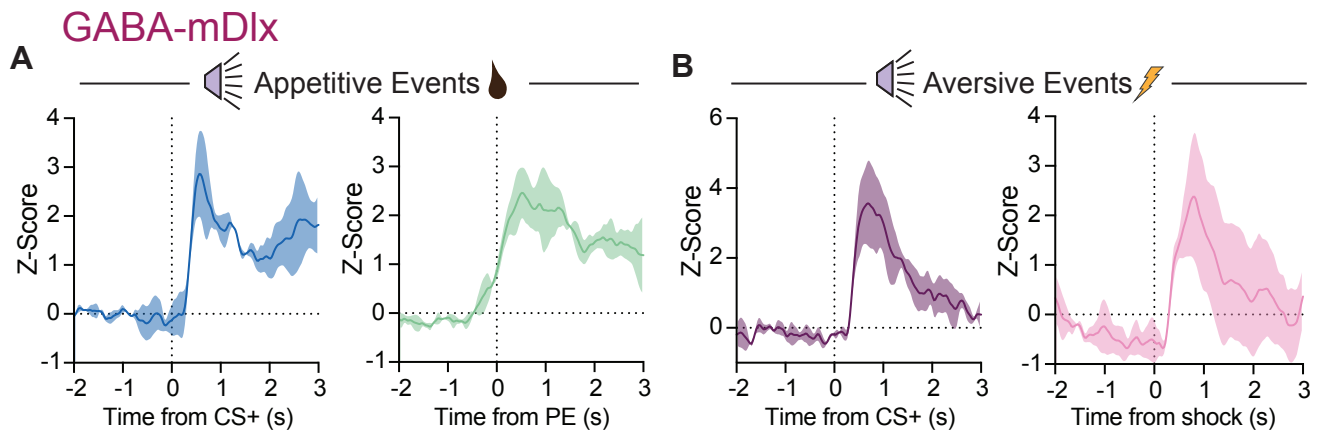
Supplemental Fig 4 | VTA mDlx neurons are similarly responsive to appetitive and aversive events

GCaMP was targeted to mDlx+ neurons in the VTA, another GABAergic population, followed by photometry recordings during and reward and fear conditioning (n=2). **A)** Reward and reward-predictive cues consistently activated mDlx+ VTA neurons. **B)** Shock and shock-predictive cues consistently activated mDlx+ VTA neurons.